

A Comparison Between Cold-Welded and Diffusion-Bonded Al/Cu Bimetallic Rods Produced by ECAE Process

P. Eslami, A. Karimi Taheri, and M. Zebardast

(Submitted June 12, 2012; in revised form October 2, 2012; published online May 25, 2013)

In this research, the application of equal channel angular extrusion process to produce both the cold-welded and diffusion-bonded Al/Cu bimetallic rods is assessed. The joints shear strength for both of the methods are measured and compared. The microstructure examinations were also carried out using scanning electron microscope equipped with EDX system and x-ray diffraction analysis. The results exhibit that the strength of the bond in cold-welded specimens is dependent on the amount of stretch and pressure at the materials interface. But in the diffusion-bonded specimens, it is depended on the struggle between the oxidation rate of the mating surfaces accompanied by inter-metallic compounds formation and the aluminum and copper atoms ability to diffuse in the joint interface.

Keywords bimetallic rod, cold welding, diffusion bonding, equal channel angular extrusion

1. Introduction

Al/Cu bimetal composite rods are used in a wide variety of electricity transmission systems and aerospace structural applications due to their unique performances (Ref 1–6). A newly introduced application of bimetallic materials is related to bus-bars (Ref 7, 8). A bus-bar is essentially a metallic bar (mostly copper) used in electronics to carry a large current and to make common connections between several circuits. A copper made bus-bar is difficult to treat because of its own heavy weight (Ref 9). Therefore, copper clad aluminum bus-bars were developed. They offer economic and weight saving advantages over solid copper. It has been reported that in comparison with a Cu rod, the bimetallic rod is 40–60% lighter and 30–40% cheaper (Ref 10, 11).

Al/Cu bimetallic rods production by cold and hot rolling processes has widely been investigated so far (Ref 12–15). Abbasi et al. (Ref 16) produced Al/Cu bimetallics by cold roll welding process and tried to investigate the growth rate of inter-metallic compounds in the materials interface. They also compared their results with a similar study on friction welding of Al to Cu and concluded that the growth rate of inter-metallic compounds in roll-welded bimetallic composites is lower than that of the similar friction welded specimens. Dyja et al. (Ref 15) provided a theoretical and experimental analysis of the rolling process of the Cu–Al bimetallic

rods. They concluded that a correctly performed rolling process assures the bimetallic rod product to be obtained with a bonding quality comparable with a stock material after explosive welding. They also compared their results for homogeneous and Al/Cu bimetallic cold rolled rods. Sheng et al. (Ref 17) investigated the influence of heat treatment on the interface of Cu/Al bimetal composite rods. They reported that a heat treatment procedure of 573 K and 20 h yields the optimum bond strength.

Copper clad aluminum bus-bar is typically produced by hydrostatic extrusion process and consists of a solid core of electrical grade aluminum with a pressure-bonded outer layer of high conductivity copper (Ref 18). When discussing different extrusion processes, equal channel angular extrusion (ECAE) is a unique one (Ref 19). ECAE is an extrusion process developed in the early 1990s in the Soviet Union (Ref 20, 21). The technique is able to refine the microstructure of metals and alloys, thereby improving their strength according to the Hall-Petch relationship (Ref 22–24). ECAE is unique because significant cold work can be accomplished without reduction in the cross-sectional area of the deformed workpiece. In conventional deformation processes like rolling, forging, extrusion, and drawing, strain is introduced by reduction in the cross-sectional area. ECAE produces significant deformation strain without reducing the cross-sectional area. This is accomplished by extruding the workpiece around the corner of two intersecting channels. The cross section of the channel is equal on entry and exit (Ref 25, 26). The complex deformation of the metal as it flows around the corner produces very high strain. Extended details about how to carry out the process and the effective parameters has been adequately described elsewhere (Ref 27–34).

ECAE process has been effectively introduced as a practical process to produce bimetallic rods over the past decade (Ref 19, 35, 36). Production of Al/Cu bimetallic rods by ECAE process can best be dealt with two different approaches. (a) Combining the ECAE process with the cold welding process principles. (b) Combining the ECAE process with the diffusion welding process principles. To compare and contrast these two approaches better, it is necessary to have a brief definition of them.

P. Eslami, A. Karimi Taheri, and M. Zebardast, Department of Materials Science and Engineering, Sharif University of Technology, Azadi Ave., P.O. Box 11365-9466, Tehran, Iran. Contact e-mails: peyman_eslami@alum.sharif.edu and ktaheri@sharif.edu.

Table 1 Specifications of the base materials

Material	Chemical Co.	Temper	σ_y , Mpa	σ_{UTS} , Mpa	Hardness, HB
Al	99.5 Al	Annealed	32	75	22
Cu	99.95 Cu	Annealed	70	220	45

Table 2 Dimensions of the components (in mm)

Group	Material	Position	Geometrical dimensions		
			Length	Diameter	Thickness
A	Al	Core	70	8.95	...
	Cu	Sheath	70	14.9	3
B	Al	Core	70	10.95	...
	Cu	Sheath	70	14.9	2
C	Al	Core	70	12.95	...
	Cu	Sheath	70	14.9	1

Cold welding is a solid state welding process in which two workpieces are joined together at room temperature and under a pressure, causing a substantial deformation of the welded parts and providing an intimate contact between the welded surfaces (Ref 37–41). On the other hand, in diffusion welding the metals are joined by causing the coalescence of the metallic surfaces during the application of pressure at an elevated temperature for a finite interval. As it becomes clear, the main differences between the two methods are related to the working temperature and extent of deformation occurring in the mating surfaces of welded parts (Ref 42–44).

In the present work, Al/Cu bimetallic rods were produced by using both of the approaches discussed above. The experiment was performed on specimens with different copper sheath thicknesses. The joints shear strength was measured and the results were compared to each other. The microstructures near the interface of diffusion-bonded Al/Cu dissimilar materials were analyzed using a scanning electron microscope (SEM) equipped with EDX system. The phase constitution in the Al/Cu diffusion zone was also analyzed by x-ray diffraction (XRD). This research is helpful to improve the shear strength and microstructure performance of the joints and to open new possibilities to produce Al/Cu bimetal composite rods.

2. Experimental Procedure

Table 1 presents the composition and mechanical properties of the materials used in this research. A cold composite rod comprising a preformed core of aluminum surrounded by a close fitting sheath of copper was prepared according to the dimensions presented in Table 2. Composite rod was obtained by cutting and machining the external surface of a billet of aluminum and the internal surface of a copper tube so that the billet is a close fit in the tube.

Afterwards, the mating surfaces of the billet and the tube were mechanically and chemically cleaned to remove substantially all oxides and other contaminating films from these surfaces. To achieve an intimate metal to metal contact it is of utmost importance that the bonding surfaces to be free from both absorbed contaminants and oxides (Ref 45). This aim was achieved by degreasing

the parts in an acetone solution, wire brushing the mating surfaces, and finally purging the external surface of the aluminum core and the internal surface of the copper sheath with nitrogen as a non-oxidizing gas, during the assembly of the two components to form the composite structure. The interval time between the surface preparation and ECAE exertion was kept less than 2 min to avoid the formation of a thick and continuous oxide layer on the mating surfaces (Ref 16, 19). The process of wire brushing the mating surfaces has been schematically shown in Fig. 1.

The aluminum core fitted into the copper sheath with a small hand force, as it was predicted in the machining precision considerations. ECAE was conducted on the billets using a die of 14.8 mm diameter channel, with a 120° channel intersection angle (θ) and a curvature of 0° on the outer side of channel intersection (ψ). Other technological parameters were as follows: (i) A split configuration die design to facilitate easy removal of the extruded specimen. (ii) A 100 ton capacity hydraulic press. (iii) MoS₂ as lubricant during pressing (Ref 46). An embracing furnace was also designed so that it could entirely encompass the ECAE die.

In the first set of experiments the ECAE process was conducted on the Al/Cu composite rods at room temperature to produce the cold-welded joints. In the second set of experiments all of the parameters remained the same, except that the ECAE process was stopped after pressing 2/3 of the specimen length. Subsequently, the die and the specimens were heated up to an elevated temperature by means of the embracing furnace described before. All of these were done while maintaining a constant ECAE pressure on the specimen. Finally, the whole system was timed to achieve a diffusion bond at the metals interface. The test was repeated for various bonding temperatures and holding times.

In order to evaluate the strength of the joints, a type of shear strength test was developed in accordance with ASTM F 1044-87 standard. The test was conducted utilizing a Hounsfield HK10S electronic universal testing machine. An especial fixture with punch and matrix switching functionality was also designed to apply the conditions stated in the standard. Shear strength test specimens were prepared perpendicular to the axial direction by a 0.01 mm precision wire cut machine. Figure 2(a), (b), and (c) shows the design of the fixture, punches and matrixes to test specimens with different copper sheath thicknesses, and a sample shear strength test specimen, respectively. Three samples in each condition were tested and the average value was reported.

To assess the mating surfaces topography, 10 mm height cylindrical specimens were cut from the produced bimetal composite rods and divided into four equal slices. Subsequently, the aluminum core was split from the copper sheath by striking a blow in the cylinder axial direction according to the trend presented in Fig. 3. The split surfaces were examined by SEM. Chemical composition alternations among the bonding interface was also analyzed by EDX system. The phase constitution near the Al/Cu interface was investigated by means of XRD analysis.

3. Results and Discussion

3.1 Shear Strength Test Results

As the first examination, in order to show that the contact between the layers is not just a mechanical lock, test samples were divided into four pieces as shown in Fig. 4. It was observed that the components were still bonded to each other

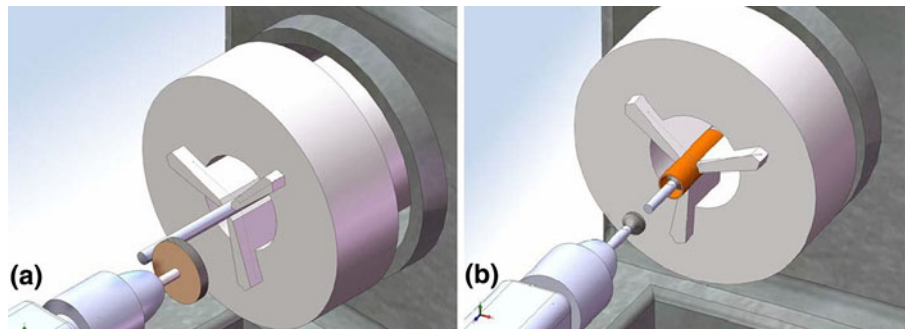


Fig. 1 Wire brushing the (a) Outer surface of the aluminum rod, (b) inner surface of the copper sheath

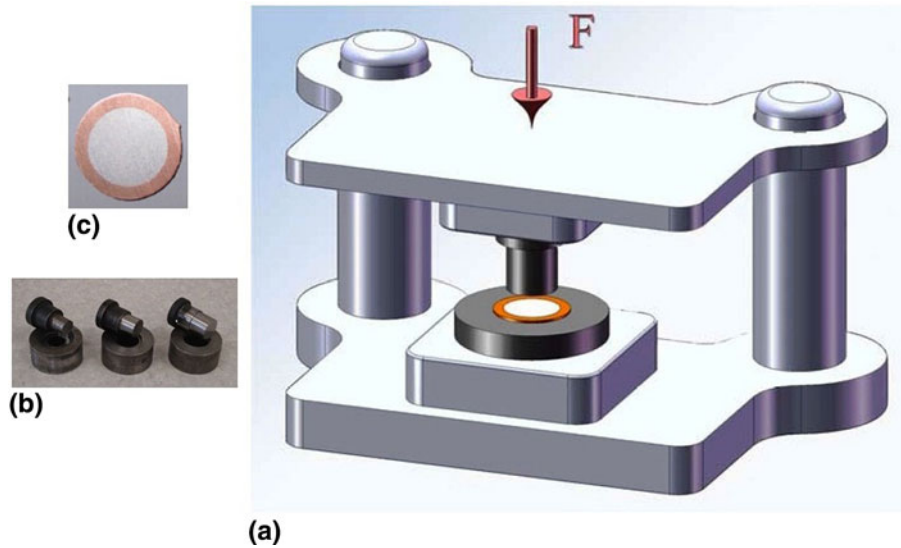


Fig. 2 (a) Shear strength test fixture, (b) shear strength test punches and matrixes, (c) shear strength test sample

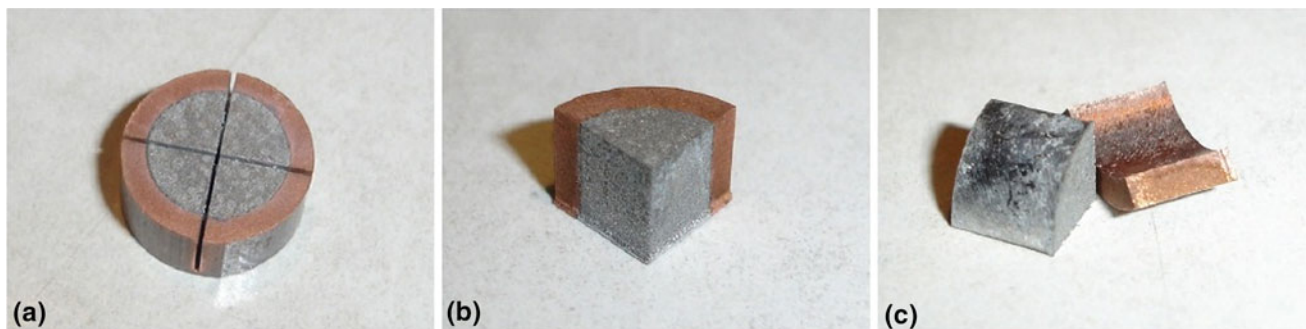


Fig. 3 The preparation stages of the topography analysis specimen

after being divided, demonstrating a weld formation between the sheath and the core.

Experimental conditions and joint shear strength results for diffusion-bonded joints are presented in Table 3. As it can be seen, there are no values presented in the table under certain time and temperature combinations due to insufficient bonding temperature to cause diffusion of atoms or insufficient holding times to achieve a sound bond. It is also obvious that a bonding temperature of 200 °C with a holding time of 60-80 min yields the highest shear strength value.

The average shear strength values of the diffusion-bonded joints versus holding times at constant bonding temperatures are shown in Fig. 5. Referring to this figure, for all bonding temperature schedules, the joint shear strength increases with increasing the holding time. However, after a specific time, degradation of this increasing trend is observed to the extent that after a short time the shear strength values remain constant with further increase in holding time.

Figure 6 shows the diffusion-bonded joints shear strength versus bonding temperatures at constant holding times. As it is

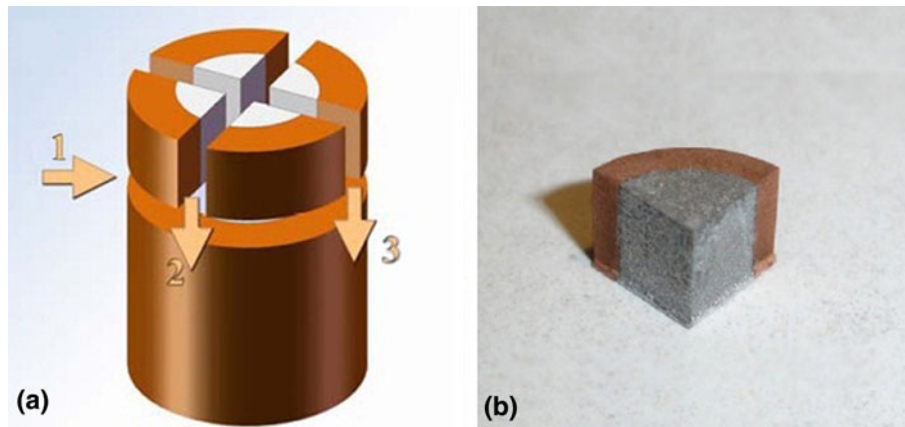


Fig. 4 Examining the weld formation between the layers (a) cutting order, (b) a quarter of the welded specimen

Table 3 Experimental conditions and diffusion-bonded joint shear strength results

Bonding condition		
Temperature, °C	Time, min	Shear strength, MPa
100	20	...
	40	...
	60	...
	80	...
	100	...
125	20	...
	40	...
	60	...
	80	...
	100	19.4
150	20	...
	40	...
	60	21.3
	80	23.3
	100	26.6
175	20	...
	40	22.3
	60	23.3
	80	27.2
	100	27.7
200	20	25.2
	40	31.1
	60	34.9
	80	34.9
	100	34.9
225	20	26.2
	40	32
	60	33.9
	80	33.6
	100	33.9

seen, almost in all of the joints fabricated, at a constant holding time, the joints shear strength increases to a maximum value with increasing the bonding temperature. Further increase in bonding temperature results in the joint shear strength degradation.

Shear strength test results for cold-welded joints and optimum diffusion-bonded ones ($T = 200\text{ }^{\circ}\text{C}$, $t = 80\text{ min}$) are compared in Fig. 7. According to this figure, it can be seen that for a constant copper sheath thickness, the joint shear strength

values for diffusion-bonded joints are more than the cold-welded ones. This trend can best be described by considering the effect of temperature. Diffusion bonding and cold welding processes both are categorized among solid state welding processes (Ref 24). The main difference between the two processes is the working temperature. Another trend which is observable in Fig. 7 is that the joint shear strength increases by an increase in the copper sheath thickness. This trend occurs for both, diffusion-bonded and cold-welded Al/Cu bimetallic rods. When the copper sheath thickness is small, the joint interface is nearer to the die wall. Subsequently, the friction between the die wall and the copper sheath affects the joint interface, significantly. As a result, the aluminum core flows with a higher velocity. This effect decreases with increasing the copper sheath thickness. Therefore, higher joint shear strength values are obtainable using a thicker copper sheath. However, a very thick copper layer leads to the rapprochement of the materials interface to the symmetry axis of the aluminum core which may decrease the bond strength (Ref 47).

Another justification that can be provided for increasing the joint shear strength by increasing the copper sheath thickness is related to the pressing force alternations. In general, one of the main factors affecting the ECAE pressure is the material to be extruded. The pressure needed to extrude a copper rod is approximately twice as much as an aluminum rod (Ref 36). This is due to the higher flow stress and work hardening coefficient of copper compared to aluminum. Accordingly, by increasing the volume ratio of copper to aluminum in a Cu/Al bimetallic rod, the ECAE pressure increases regardless of the type and the amount of the applied strain. Increased ECAE pressure increases the pressure between the layers. More pressure between the layers means more surface asperities entanglements which can improve the metals contact area and provides more locations with a chance to form a bond.

3.2 Analysis of Materials Flow and Strain Distribution

In general, radial strain in ECAE of an Al/Cu bimetal rod is more uniform than that of a mono-metal rod of aluminum and copper. Since the stress which is applied to the material in the vicinity of die wall is larger than the stress near the axis of symmetry, more radial strain is produced in the outer layers of mono-metal rods. However, in a bimetal Al/Cu rod, the larger stresses in the vicinity of die wall are applied to the harder sheath material and the lower stresses near the axis of symmetry

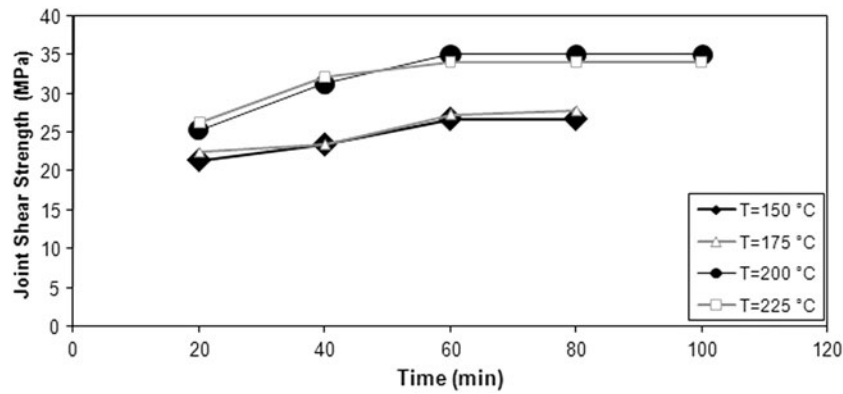


Fig. 5 Diffusion-bonded joint shear strength vs. holding time at constant bonding temperatures

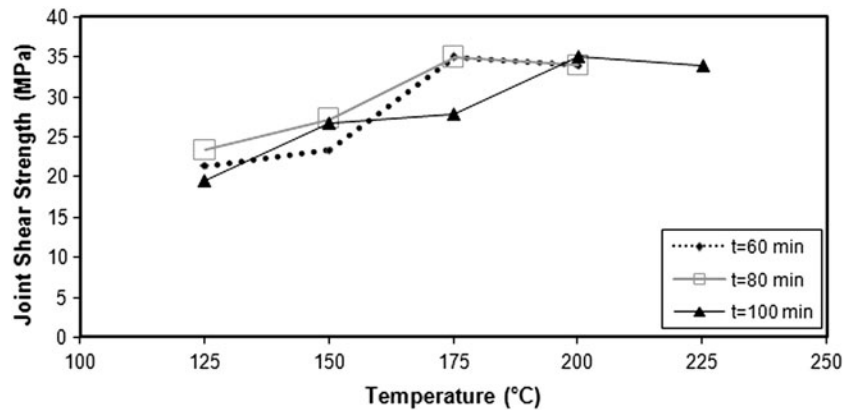


Fig. 6 Diffusion-bonded joint shear strength vs. bonding temperature at constant holding times

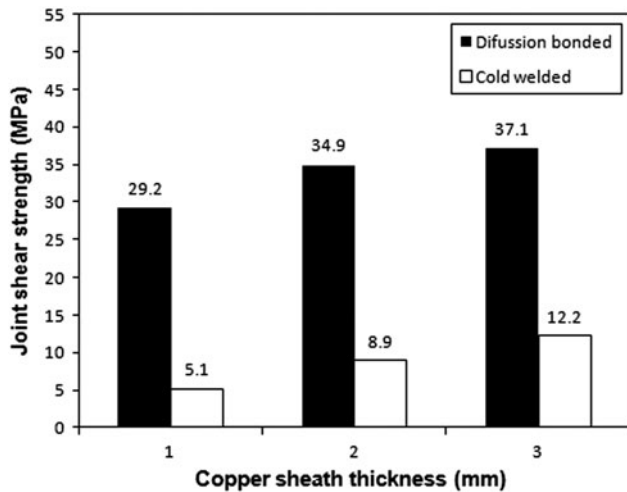


Fig. 7 Shear strength of joints vs. copper sheath thickness

are applied to the softer core material. As the result, a more uniform distribution of radial strain is obtained in a bimetal rod. Beside this, the compressive stress inside the die may lead to creation of bonds at the interface only when the two metals flow with the same velocity in the vicinity of their interface. Thus, velocity distribution is the dominant factor in formation of a sound bond at the materials interface.

A major concern in this research was the probable non-uniform deformation of the components in the ECAE die, due

to the different flow characteristics of aluminum and copper. This non-uniformity could result in an inadequate contact between the mating surfaces to form sound bonds. Figure 8(a) shows the conditions of materials flow from the starting point of the extrusion process till the end. The first stage includes the entrance of the bimetallic rod into the input channel of the die. In this stage, the bimetal rod places at the lowest possible point of the input channel. The bimetal rod would not go below this point without pressure. By exerting pressure from above by the mandrel rod, the bimetal rod begins to deform and fills the die channel space. Part of the deformation is along the radius and in the cross section of the bar which brings the bar in a close contact with the die wall and eliminates the air gap between the Al/Cu layers. Simultaneously, another part of the deformation occurs at the lower part of the bar which fills the space available in the die channels intersection point. This filling is along with the flow of some material to the output channel (Fig. 8b).

With continued pressure, the materials begin to enter the output channel. But the flow does not occur in all parts equally. The $\Psi = 0^\circ$ of the die used in this research, leads to the formation of a dead zone at the outer side of the channels intersection area. Thus, material flow occurs with a delay in this area. This phenomenon is not recognizable when conducting ECAE on a mono-metal rod, due to the continuity in both the matter and the color of the rod. But in case of a bimetallic rod, a different flow behavior is clearly detectable in the materials shear zone. Formation of the dead zone results in a different flow velocity of the aluminum core from the copper sheath. In

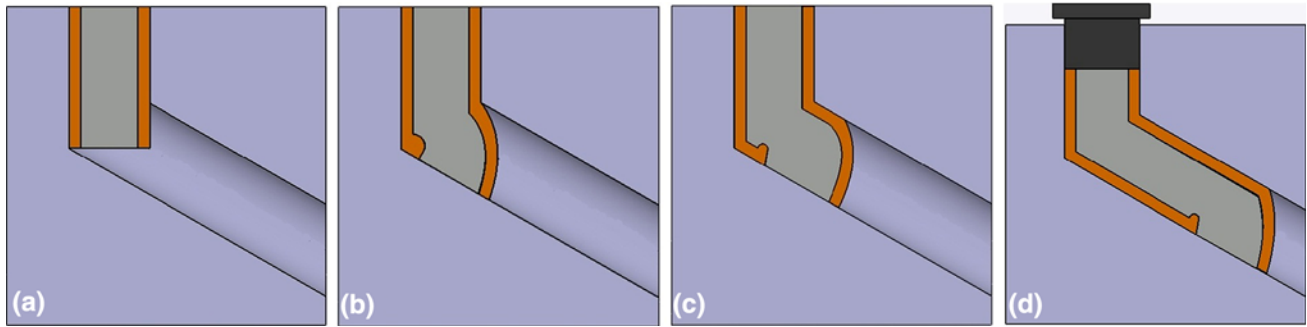


Fig. 8 The bimetal rod flow stages in the ECAE die

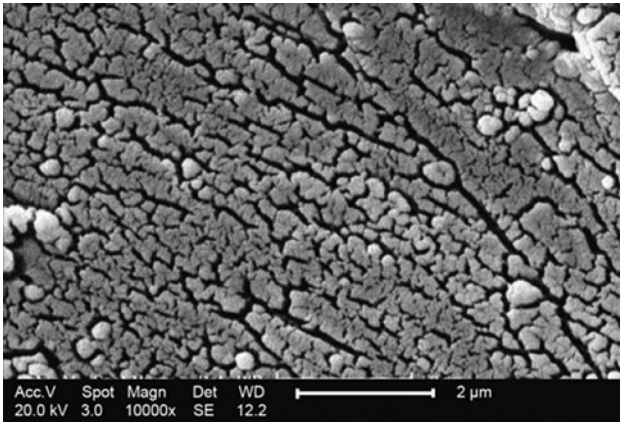


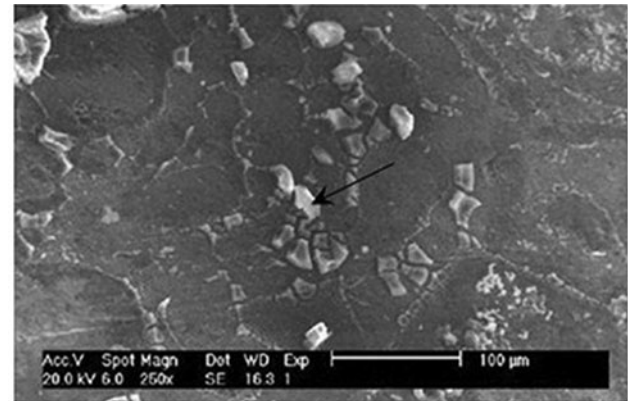
Fig. 9 SEM image of the split aluminum surface of the cold-welded joint

addition, the inability of the copper layer to flow into the output channel along with the pressure exerting by the mandrel rod, leads to the accumulation of copper and a kind of non-uniformity in the flow of the bimetal rod. This non-uniformity shows itself with a retardation of the copper sheath from the aluminum core in the produced bimetallic rod.

In the last stage, as presented in Fig. 8(c), after a delay in the flow of copper, this layer also leaves the dead zone and extrudes into the exit channel. From this point on, the flow process occurs uniformly and without any delays throughout the slip plane. At this stage, if the copper layer desires to show a non-uniform flow, it has to become thicker in its region of non-uniformity. If this thickness increase occurs in the shear zone, the aluminum rod thickness must decrease in the same region, in response. Consequently, the amount of mass that has been decreased in the aluminum layer has to be transferred to the other parts of the bar. This mass transfer cannot occur in the input channel of the die, since the bar is under the mandrel pressure at that point. Thus, the only remaining way is to transfer the mass to the output channel at the end side of the bar. But the copper wall formed in front of the layers, as shown in Fig. 8(d), prevents any slip of the layers or change in the aluminum rod thickness. Consequently, neither thickness changes, nor non-uniform flow occurs in the shear zone of the materials.

3.3 SEM analysis of split surfaces

Figure 9 shows the split aluminum surface of the cold-welded joint. In this figure, an extensive network of cracks is



Element	Weight%	Atomic%
O	43.15	58.21
Al	48.91	39.08
Cu	7.86	2.63

Fig. 10 SEM image of split aluminum surface of the joint produced at 150 °C with a holding time of 100 min

observable on the aluminum surface. The brushing process in the surface preparation stage, leads to the formation of a number of grooves and peaks in the surface. This happens because of the detachment of material from the surface during brushing. In other words, brushing creates a thin severely deformed, and therefore work-hardened layer on the material surface. This layer is very brittle. In the extrusion stage, these brittle layers break up at the materials interface as a result of the surface stretch produced, and a network of cracks forms on the materials surface. The depth of the cracks is proportional to the work-hardened layer thickness. Subsequently, the virgin metals begin to extrude through the cracks to form a bond between the mating surfaces. Therefore, it is expected that the strength of the bond in cold-welded specimens to be depended on the amount of stretch and pressure at the materials interface.

This observation is completely in accordance with the accepted theory known as the “film theory” introduced for the first time by Vaidyanath et al. (Ref 48) to describe the predominant mechanism in a pressure cold weld formation. The theory is based on breaking up the mating surfaces of the layers during the process and extruding the virgin metals through the cracks. According to this mechanism, there is a threshold amount of deformation after which cracks perpendicular to the pressing direction appear in the layers. Cracks propagation allows the bond to establish between the virgin metals at their mating surfaces.

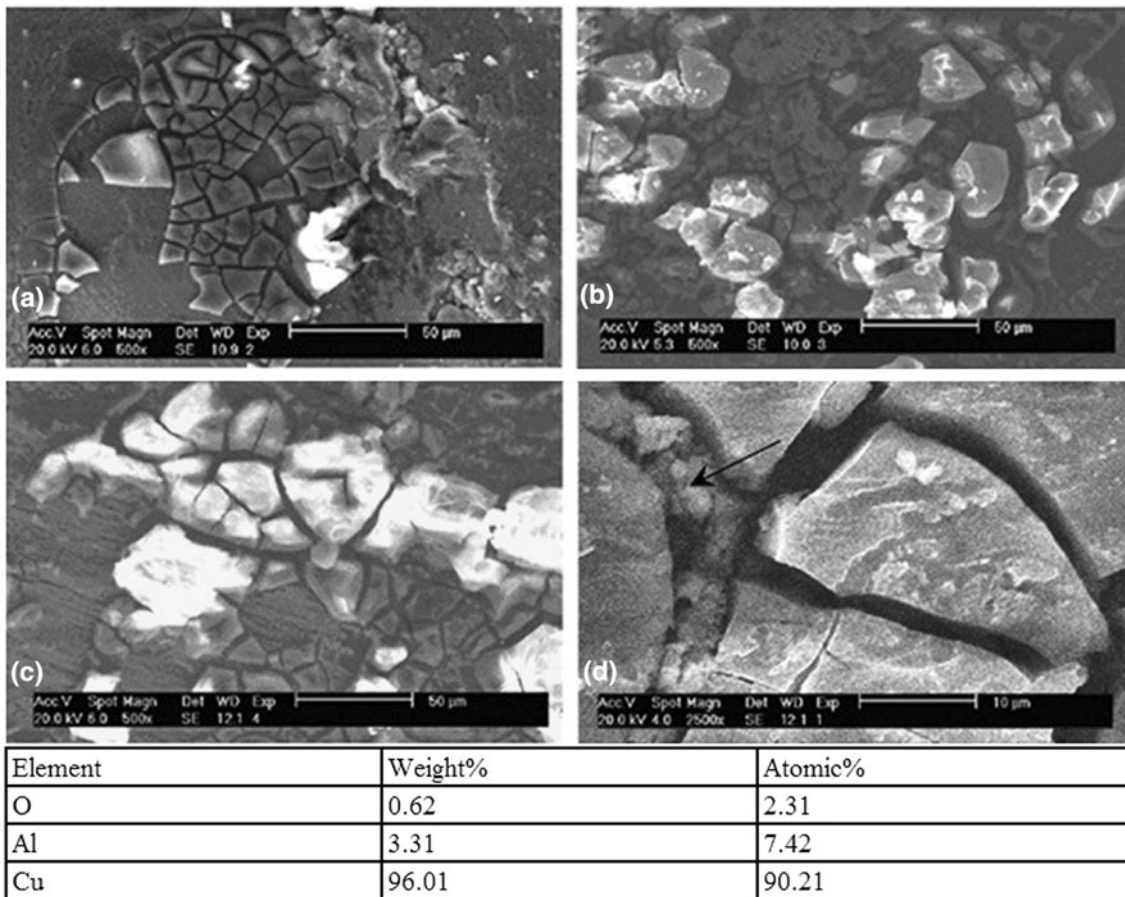


Fig. 11 SEM images of split aluminum surface of the joints produced at (a) 175 °C, (b) 200 °C, (c, d) 225 °C with a holding time of 100 min

The split aluminum surface of the diffusion-bonded joint produced at 150 °C with a holding time of 100 min is presented in Fig. 10. Referring to this figure, there are scattered particles with low congregation observable on the aluminum surface. The spot analysis obtained from one of these particles revealed the oxide nature of the particles, since the aluminum and oxygen atomic percents were approximately correspondent to the Al_2O_3 stoichiometric proportions. Since the raw materials used in this research have a purity of more than 99%, the spot analysis results are limited to three major elements including aluminum, copper, and oxygen. The amount of impurities was neglected to simplify the data analysis and comparison of the results.

Figure 11(a), (b), and (c) exhibit the split aluminum surface of the diffusion-bonded joints produced at bonding temperatures of 175, 200, and 225 °C at a constant holding time, respectively. As it can be seen in these figures, the oxide particles thickness and extension are increased by increasing the bonding temperature. On the other hand, by increasing the bonding temperature, further diffusion of copper among the ruptured oxide layer is observable in Fig. 11(d). The spot analysis of the particles settled in oxide layer ruptures clearly proved this fact.

Referring to the joints shear strength results presented in Table 3 and the SEM pictures of the split surfaces of the diffusion-bonded joints, it seems that the acceleration of oxide layer formation by increasing the bonding temperature from 150 to 200 °C, not only does not cause a degradation of the joint shear strength, but also a tangible increase in the values are observed. This could be restated in this way; the diffusion

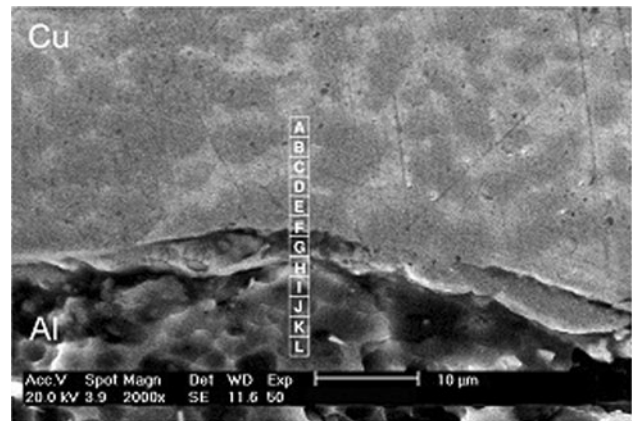


Fig. 12 contiguous points at the diffusion-bonded joint interface analyzed by EDX

of the materials at their mating interface by the augmentation of the bonding temperature, predominates the oxide layer formation and its harmful effects up to 200 °C, and the general joint shear strength value increases by multiplying the diffusion-bonded sites. Eventually, by reaching the bonding temperature to 225 °C, an almost continuous oxide layer forms on the aluminum surface which prevents proper diffusion of atoms in the materials interface. This thick continuous oxide layer is brittle initially and weakens the bond quality.

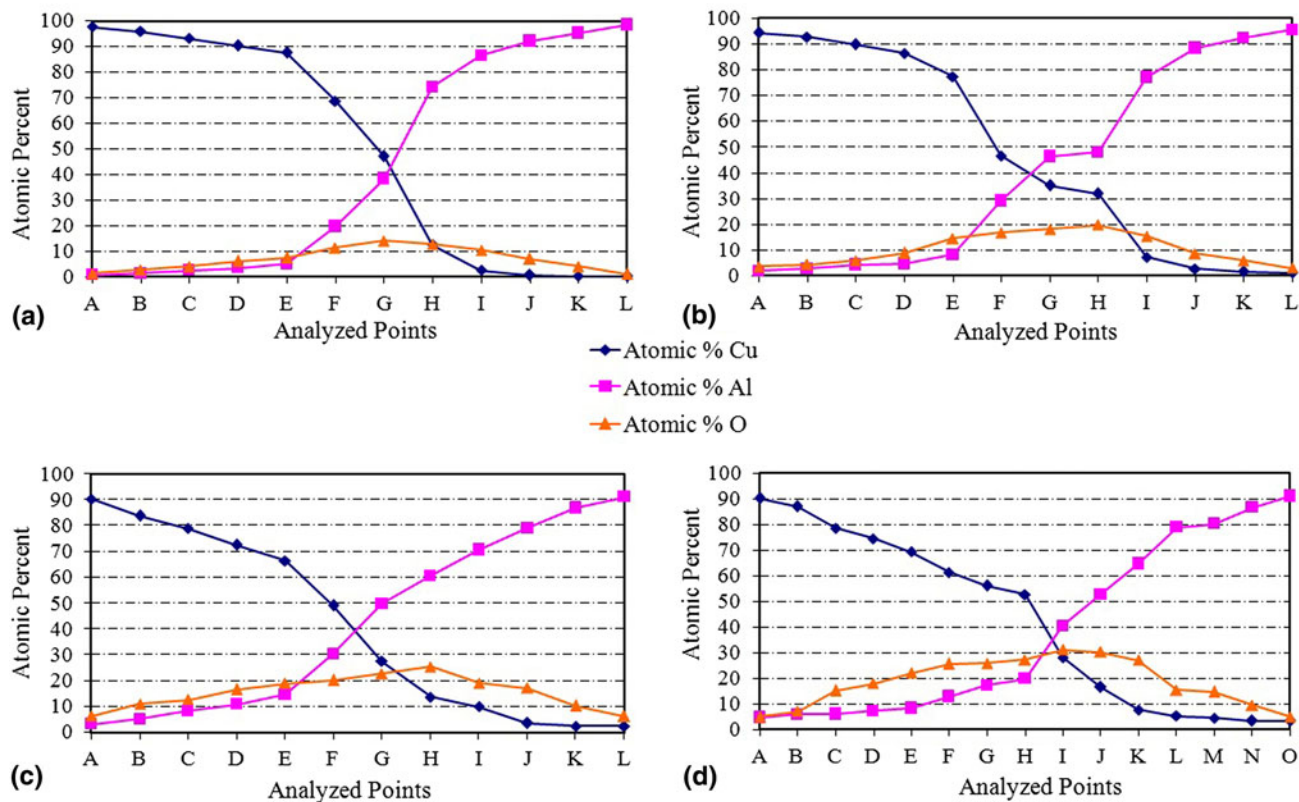


Fig. 13 Atomic percent of Al, Cu and O vs. analyzed points for the joints produced with a holding time 100 min at (a) 150 °C, (b) 175 °C, (c) 200 °C, (d) 225 °C

3.4 EDX analysis

The interface region of the diffusion-bonded joints was analyzed at contiguous points standing at 1.5-2 μm distance from each other (Fig. 12).

Diagrams of the atomic percent of the main elements (Al, Cu, O) versus the analyzed points for the joints produced at various temperatures are presented in Fig. 13. According to this figure, the oxygen curve is shifted up by increasing the bonding temperature. This is due to the higher rate of oxidation at elevated temperatures. Moreover, at all bonding temperatures the maximum in oxygen curve occurs in a region adjacent to aluminum. This is caused due to the fact that aluminum is a more active metal compared to copper, and has a higher oxygen absorption tendency.

It is interesting to note that although the maximum in the oxygen curves occurs in a region adjacent to aluminum, the diffusion range of oxygen atoms in aluminum is lower compared to that in copper. In other words, the oxygen curve experiences an intense slope in aluminum region compared to copper. In fact, the formation of a compact and continuous oxide layer on the aluminum surface makes it difficult even for the small oxygen atoms to diffuse in subsurface layers. On the contrary, the non-continuous oxide layer on the copper surface allows an enhanced diffusion of the oxygen atoms in its matrix.

In a general view, at a same distance from the joint interface, the aluminum atomic percent in copper matrix is higher than that of copper in aluminum matrix. There are two reasons to explain this phenomenon. First, the diffusivities of different species are not the same in a diffusion couple due to the Kirkendall effect. Atoms of the element with a lower melting point exhibit a higher

diffusivity compared to that of the atoms of the element with a higher melting point. Since the melting point of aluminum is lower than that of copper, the diffusion range of aluminum atoms would be higher in a fixed distance in copper matrix compared to that of copper atoms in aluminum matrix. Second, the continuous oxide layer on the aluminum surface, as mentioned before, hinders proper diffusion of copper atoms in the aluminum matrix.

3.5 XRD analysis

The interface of solid state welded Al/Cu is susceptible to the nucleation and growth of inter-metallic compounds at temperatures greater than 120 °C (Ref 35, 42). This is a thermally activated process and by increasing the temperature the nucleation and growth of inter-metallic compounds and formation of oxide layers are accelerated (Ref 49). These compounds have a non-metallic covalence bond and therefore are brittle and can weaken the bonding strength (Ref 16, 50). Therefore to investigate the existence of such compounds at the materials interface and to identify their type, and finally to take advantage in explaining the joint shear strength values variations, the Al/Cu diffusion interface was analyzed by XRD method.

From the Al-Cu constitution diagram, it follows that in this system there are a number of chemical compounds which are stable at room temperature, namely, the θ-phase (CuAl₂), η-phase (CuAl), ξ₂-phase, δ-phase (Cu₃Al₂), and γ₂-phase (Cu₂Al). Jin et al. (Ref 51) reported that AlCu and Al₂Cu were the main phases in the Al/Cu bonds based on micro-XRD analysis results at temperatures from 150 to 200 °C. Kim et al. (Ref 52) also used the micro-XRD to identify the Al/Cu inter-metallic compounds phases on fractured pads and balls after

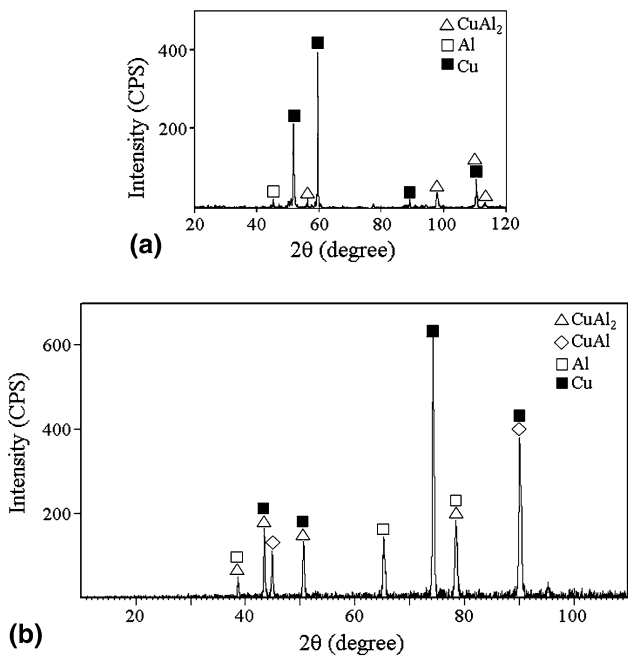


Fig. 14 XRD results for the joints produced at (a) 200 °C, (b) 225 °C with a holding time of 100 min

ball shear testing. They have reported that Cu_9Al_4 was the main phase at the temperature range from 150 to 300 °C.

In present research, the XRD results of the phase constituents in the diffusion-bonded Al/Cu interface produced at bonding temperatures of 200 and 225 °C with a holding time of 100 min, are shown in Fig. 14(a) and (b), respectively.

According to these results, the Al/Cu interface zone diffusion-bonded at 200 °C consists of CuAl_2 phase. Figure 10(b) shows that, by increasing the bonding temperature to 225 °C, the CuAl phase is detected in addition to CuAl_2 . As a matter of fact, the strength of the bond decreases with increasing the inter-metallic width. The inter-metallic compounds are brittle phases and there is a critical width at which the bond strength reduces. Abbasi et al. (Ref 16) have reported this critical width as 2.5 μm for the heat-treated Al/Cu bimetal composite produced by cold roll welding. It can be deduced that the decrease in the joint shear strength at bonding temperature of 225 °C compared to the joint produced at 200 °C is due to the nucleation of new inter-metallic phases and also the growth of the formerly existing inter-metallic phases to a critical width. These results distinctly indicate that the bonding mechanism is related to the struggle between the mating surfaces oxidation rate accompanied by the formation of inter-metallic compounds as well as the ability of the aluminum and copper atoms to diffuse in the joint interface. Both of these factors are amplified by increasing the bonding temperature. The former is detrimental and the latter plays a constructive role in the joint formation. Hence, the final joint quality is dependent on the extent that the diffusion of the atoms dominates the formation of the oxide layer and inter-metallic compounds.

4. Conclusion

Al/Cu bimetal composite rods were produced by conducting ECAE combined with cold welding and diffusion bonding

processes. The joints shear strength for both of the methods were measured and compared. The microstructure and phase constitution near the diffusion bonding interface of Al/Cu bimetal composite rods were studied and the results were used to explain the joint shear strength values fluctuations. The following conclusions were made from the results:

1. ECAE process can be effectively used to produce cold-welded and diffusion-bonded aluminum-copper bimetallic rods.
2. In a constant copper sheath thickness, the joint shear strength values for diffusion-bonded joints are more than the cold-welded ones.
3. The joint shear strength increases by increasing the copper sheath thickness, regardless of the joining technique being used.
4. A bonding temperature of 200 °C with a holding time of 60-80 min yields the highest shear strength value for diffusion-bonded joints.
5. The strength of the bond in cold-welded specimens is dependent on the amount of stretch and pressure at the materials interface. But in the diffusion-bonded specimens, the bonding mechanism is related to the struggle between the mating surfaces oxidation rate accompanied by inter-metallic compounds formation and the aluminum and copper atoms ability to diffuse in the joint interface. The former is detrimental and the latter plays a constructive role in the formation of joint.

Acknowledgments

The authors would like to thank the Iran National Science Foundation (INSF) and the Research Board of Sharif University of Technology for the financial support and the provision of the research facilities used in this work.

References

1. H. Papkala and A. Pietras, Pressure Welding of Aluminium to Copper, *Weld. Int.*, 2006, **20**(3), p 173–182
2. P. Liu, Q. Shi, W. Wang, X. Wang, and Z. Zhang, Microstructure and XRD Analysis of FSW Joints for Copper T2/Aluminium 5A06 Dissimilar Materials, *Mater. Lett.*, 2008, **62**(25), p 4106–4108
3. Y. Guo, G. Qiao, W. Jian, and X. Zhi, Microstructure and Tensile Behavior of Cu-Al Multi-layered Composites Prepared by Plasma Activated Sintering, *Mater. Sci. Eng. A*, 2010, **527**(20), p 5234–5240
4. A. Abdollah-Zadeh, T. Saeid, and B. Sazgari, Microstructural and Mechanical Properties of Friction Stir Welded Aluminum/Copper Lap Joints, *J. Alloys Compd.*, 2008, **460**(1–2), p 535–538
5. M. Eizadjou, A. Kazemi Talachi, H. Danesh Manesh, H. Shakur Shahabi, and K. Janghorban, Investigation of Structure and Mechanical Properties of Multi-layered Al/Cu Composite Produced by Accumulative Roll Bonding (ARB) Process, *Compos. Sci. Technol.*, 2008, **68**(9), p 2003–2009
6. S. Madhusudan, M.M.M. Sarcar, and N.R.M.R. Bhargava, Fabrication and Characterization of Aluminium-Copper Composites, *J. Alloys Compd.*, 2009, **471**(1–2), p 116–118
7. W.E. Verkamp, Copper-to-Aluminum Transitions in High DC Bus Systems, *IEEE Trans. Ind. Appl.*, 1997, **33**(4), p 1027–1034
8. M. Braunovic, and N. Aleksandrov, Effect of Electrical Current in Bimetallic Aluminum-Copper Joint, *IEEE Trans. Paper No. CHMT-93-10*, 1993, p 261–268

9. T.-G. Zhou, Z.Y. Jiang, J.L. Wen, and A.K. Tieu, A Method to Produce Aluminum Alloy Tube Busbars by Continuous Casting-Expansion Extrusion, *J. Mater. Process. Technol.*, 2006, **177**(1–3), p 163–166
10. A. Khosravifard and R. Ebrahimi, Investigation of Parameters Affecting Interface Strength in Al/Cu Clad Bimetal Rod Extrusion Process, *Mater. Des.*, 2010, **31**(1), p 493–499
11. T.T. Sasaki, R.A. Morris, G.B. Thompson, Y. Syarif, and D. Fox, Formation of Ultra-Fine Copper Grains in Copper-Clad Aluminum Wire, *Scripta Mater.*, 2010, **63**(5), p 488–491
12. Z.-C. Lin and T.-G. Huang, Hot Rolling of an Aluminum-Copper Sandwich Flat Strip with the Three-Dimensional Finite Element Method, *J. Mater. Process. Technol.*, 2000, **99**(1–3), p 154–168
13. W. Lehnert and N.D. Cuong, Experimental and Mathematical Simulation of Microstructural Evolution During Hot Rolling of Al and Cu Material, *J. Mater. Process. Technol.*, 1996, **60**(1–4), p 567–574
14. A.G. Mamalis, N.M. Vaxevanidis, A. Szalay, and J. Prohaszka, Fabrication of Aluminium/Copper Bimetallics by Explosive Cladding and Rolling, *J. Mater. Process. Technol.*, 1994, **44**(1–2), p 99–117
15. H. Dyja, S. Mróz, and A. Milenin, Theoretical and Experimental Analysis of the Rolling Process of Bimetallic Rods Cu-Steel and Cu-Al, *J. Mater. Process. Technol.*, 2004, **153–154**, p 100–107
16. M. Abbasi, A. Karimi Taheri, and M.T. Salehi, Growth Rate of Intermetallic Compounds in Al/Cu Bimetal Produced by Cold Roll Welding Process, *J. Alloys Compd.*, 2001, **319**(1–2), p 233–241
17. L.Y. Sheng, F. Yang, T.F. Xi, C. Lai, and H.Q. Ye, Influence of Heat Treatment on Interface of Cu/Al Bimetal Composite Fabricated by Cold Rolling, *Composites Part B*, 2011, **42**(6), p 1468–1473
18. H.J. Park, K.H. Na, N.S. Cho, Y.S. Lee, and S.W. Kim, A Study of the Hydrostatic Extrusion of Copper-Clad Aluminium Tube, *J. Mater. Process. Technol.*, 1997, **67**(1–3), p 24–28
19. A.R. Eivani and A. Karimi Taheri, A New Method for Producing Bimetallic Rods, *Mater. Lett.*, 2007, **61**(19–20), p 4110–4113
20. A. Sivaraman and U. Chakkingal, Flow Properties of Commercial Purity Aluminum Processed by Equal Channel Angular Pressing, *Mater. Sci. Eng. A*, 2008, **487**(1–2), p 264–270
21. A. Gholinia, P.B. Prangnell, and M.V. Markushev, The Effect of Strain Path on the Development of Deformation Structures in Severely Deformed Aluminium Alloys Processed by ECAE, *Acta Mater.*, 2000, **48**(5), p 1115–1130
22. D.J. Alexander, New Methods for Severe Plastic Deformation Processing, *J. Mater. Eng. Perform.*, 2007, **16**(3), p 360–374
23. H.G. Salem and J.S. Lyons, Effect of Equal Channel Angular Extrusion on the Microstructure and Superplasticity of an Al-Li Alloy, *J. Mater. Eng. Perform.*, 2002, **11**(4), p 384–391
24. L.D. Hefti, Advances in Fabricating Superplastically Formed and Diffusion Bonded Components for Aerospace Structures, *J. Mater. Eng. Perform.*, 2004, **13**(6), p 678–682
25. W.H. Huang, C.Y. Yu, P.W. Kao, and C.P. Chang, The Effect of Strain Path and Temperature on the Microstructure Developed in Copper Processed by ECAE, *Mater. Sci. Eng. A*, 2004, **366**(2), p 221–228
26. S. Qu, X.H. An, H.J. Yang, C.X. Huang, G. Yang, Q.S. Zang, Z.G. Wang, S.D. Wu, and Z.F. Zhang, Microstructural Evolution and Mechanical Properties of Cu-Al Alloys Subjected to Equal Channel Angular Pressing, *Acta Mater.*, 2009, **57**(5), p 1586–1601
27. V.M. Segal, Materials Processing by Simple Shear, *Mater. Sci. Eng. A*, 1995, **197**(2), p 157–164
28. R.Z. Valiev and T.G. Langdon, Principles of Equal-Channel Angular Pressing as a Processing Tool for Grain Refinement, *Prog. Mater. Sci.*, 2006, **51**(7), p 881–981
29. K. Narooei and A. Karimi Taheri, A New Model for Prediction the Strain Field and Extrusion Pressure in ECAE Process of Circular Cross Section, *Appl. Math. Model.*, 2010, **34**(7), p 1901–1917
30. A.R. Eivani, S. Ahmadi, E. Emadoddin, S. Valipour, and A. Karimi Taheri, The Effect of Deformations Passes on the Extrusion Pressure in Axi-symmetric Equal Channel Angular Extrusion, *Comput. Mater. Sci.*, 2009, **44**(4), p 1116–1125
31. Y.C. Yuan, A.B. Ma, J.H. Jiang, and D.H. Yang, Finite Element Analysis of the Deformation Distribution During Multi-Pass Rotary-Die ECAP, *J. Mater. Eng. Perform.*, 2011, **20**(8), p 1378–1384
32. A.R. Eivani and A. Karimi Taheri, The Effect of Dead Metal Zone Formation on Strain and Extrusion Force During Equal Channel Angular Extrusion, *Comput. Mater. Sci.*, 2008, **42**(1), p 14–20
33. A.R. Eivani and A. Karimi Taheri, A New Method for Estimating Strain in Equal Channel Angular Extrusion, *J. Mater. Process. Technol.*, 2007, **183**(1), p 148–153
34. C. Xu, T.G. Langdon, Z. Horita, and M. Furukawa, Using Equal-Channel Angular Pressing for the Production of Superplastic Aluminum and Magnesium Alloys, *J. Mater. Eng. Perform.*, 2004, **13**(6), p 683–690
35. P. Eslami and A. Karimi Taheri, An Investigation on Diffusion Bonding of Aluminum to Copper Using Equal Channel Angular Extrusion Process, *Mater. Lett.*, 2011, **65**(12), p 1862–1864
36. M. Zebardast and A. Karimi Taheri, The Cold Welding of Copper to Aluminum Using Equal Channel Angular Extrusion (ECAE) Process, *J. Mater. Process. Technol.*, 2011, **211**(6), p 1034–1043
37. W. Zhang and N. Bay, A Numerical Model for Cold Welding of Metals, *CIRP Ann. Manuf. Technol.*, 1996, **45**(1), p 215–220
38. M. Acarer, Electrical, Corrosion, and Mechanical Properties of Aluminum-Copper Joints Produced by Explosive Welding, *J. Mater. Eng. Perform.*, 2012, **21**(11), p 2375–2379
39. P.K. Wright, D.A. Snow, and C.K. Tay, Interfacial Conditions and Bond Strength in Cold Pressure Welding by Rolling, *Met. Technol.*, 1978, **5**(1), p 24–31
40. N. Bay, Cold Welding: Part I, Characteristic, Bonding Mechanisms, Bond Strength, *Met. Constr.*, 1986, **18**(6), p 369–372
41. T. Tabata, S. Masaki, and K. Azekura, Bond Criterion in Cold Pressure Welding of Aluminum, *Mater. Sci. Technol.*, 1989, **5**(4), p 377–381
42. G. Mahendran, S. Babu, and V. Balasubramanian, Analyzing the Effect of Diffusion Bonding Process Parameters on Bond Characteristics of Mg-Al Dissimilar Joints, *J. Mater. Eng. Perform.*, 2010, **19**(5), p 657–665
43. L.D. Hefti, Innovations in the Superplastic Forming and Diffusion Bonded Process, *J. Mater. Eng. Perform.*, 2008, **17**(2), p 178–182
44. Y. Xiang, S. Wu, and D. Chen, Fracture Toughness of Superplastic Formed/Diffusion Bonded Interfaces, *J. Mater. Eng. Perform.*, 2001, **10**(6), p 679–684
45. T.I. Khan and O. Ohashi, Effect of Argon Ion Bombardment on the Solid-State Diffusion Bonding of Copper, *Scripta Mater.*, 1998, **38**(10), p 1525–1532
46. X.G. Qiao, M.J. Starink, and N. Gao, Hardness Inhomogeneity and Local Strengthening Mechanisms of an Al1050 Aluminium Alloy After One Pass of Equal Channel Angular Pressing, *Mater. Sci. Eng. A*, 2009, **513–514**, p 52–58
47. C.G. Kang, Y.J. Jung, and H.C. Kwon, Finite Element Simulation of Die Design for Hot Extrusion Process of Al/Cu Clad Composite and Its Experimental Investigation, *J. Mater. Process. Technol.*, 2002, **124**(1–2), p 49–56
48. L.R. Vaidyanath, M.G. Nicholas, and D.R. Milner, Pressure Welding by Rolling, *Weld. J.*, 1959, **6**, p 13–28
49. W.-B. Lee, K.-S. Bang, and S.-B. Jung, Effects of Intermetallic Compound on the Electrical and Mechanical Properties of Friction Welded Cu/Al Bimetallic Joints During Annealing, *J. Alloys Compd.*, 2005, **390**(1–2), p 212–219
50. P. He and D. Liu, Mechanism of Forming Interfacial Intermetallic Compounds at Interface for Solid State Diffusion Bonding of Dissimilar Materials, *Mater. Sci. Eng. A*, 2006, **437**(2), p 430–435
51. J.O. Koizumi, M. Araki, and I. Hitachi, Investigation of the Reliability of Copper Ball Bonds to Aluminum Electrodes, *IEEE Trans. Compon. Hybrids Manuf. Technol.*, 1987, **10**(4), p 550–555
52. H.J. Kim, J.Y. Lee, K.W. Paik, K.W. Koh, J.H. Won, S.H. Choi, J. Lee, J.T. Moon, and Y.J. Park, Effects of Cu/Al Intermetallic Compound (IMC) on Copper Wire and Aluminum Pad Bondability, *IEEE Trans. Compon. Packag. Technol.*, 2003, **26**(2), p 367–374